DOI: 10.1111/jdv.18324 JEADV

ORIGINAL ARTICLE

Line-field confocal optical coherence tomography: a new tool for non-invasive differential diagnosis of pustular skin disorders

L. Tognetti,[1,*] E. Cinotti,[1,2] F. Falcinelli,[1] C. Miracco,[3] M. Suppa,[2,4,5] J.-L. Perrot,[2,6] P. Rubegni[1]

[1]Dermatology Unit and Skin Bank, Department of Medical, Surgical and Neurosciences, Siena University Hospital, Siena, Italy
[2]Groupe d'Imagerie Cutanée Non-Invasive (GICNI) of the Société Française de Dermatologie (SFD), Paris, France
[3]Department of Medicine, Surgery and Neurosciences Pathological Anatomy Section, University of Siena, Siena, Italy
[4]Department of Dermatology, Hôpital Erasme, Université Libre de Bruxelles, Brussels, Belgium
[5]Institut Jules Bordet, Université Libre de Bruxelles, Brussels, Belgium
[6]Dermatology Unit, University Hospital of St-Etienne, Saint Etienne, France
*Correspondence: L. Tognetti. E-mail: linda.tognetti@dbm.unisi.it

Abstract

Background The spectrum of pustular skin disorders (PSD) is large and particularly challenging, including inflammatory, infectious and amicrobial diseases. Moreover, although pustules represent the unifying clinical feature, they can be absent or not fully developed in the early stage of the disease. The line-field confocal optical coherence tomography (LC-OCT) is a recently developed imaging technique able to perform a non-invasive, *in vivo*, examination of the epidermis and upper dermis, reaching very high image resolution and virtual histology.

Objectives We aimed to investigate the potentialities of LC-OCT in the non-invasive differential diagnosis of a series of 11 PSD with different aetiology, microscopic features, body location and incidence rates.

Materials and Methods Complete LC-OCT imaging (i.e. 2D/3D frames, videos) was performed on a total of 19 patients (10 females and 9 males) aged between 35 and 79 years. Images were blindly evaluated and compared with corresponding histopathologic findings.

Results The LC-OCT imaging was able to detect with high accuracy the pustule structure including shape, margins, morphology and cellular content, along with peculiar epidermal and adnexal alterations in each condition, including: Acute Generalized Exanthematous Pustulosis, Generalized pustular psoriasis, Generalized pustular figurate erythema, Subcorneal Pustular Dermatosis, Intraepidermal IgA pustulosis, Palmoplantar pustulosis, Palmoplantar pustular psoriasis. Herpetic whitlow, Acrodermatitis continua of Hallopeau, Vesicopustular Sweet syndrome and Vesicopustular Eosinophilic cellulitis, with pustular appearance, were also compared.

Conclusions The new LC-OCT can represent a rapid, non-invasive and painless tool which can help differentiating among PSD of different aetiology and microscopic morphology in clinical mimickers in daily practice.

Received: 31 January 2022; Accepted: 29 April 2022

Conflicts of interest

There are no known conflicts of interests to disclose.

Funding sources

None.

Background

The spectrum of pustular skin disorders (PSD) is large and include either inflammatory, drug-induced, or autoinflammatory and infectious conditions determining the development of amicrobic or microbic pustules, respectively. Although a careful clinical history collection and detection of pathognomonic diagnostic clues can help orienting the diagnostic suspect, especially in infectious PSD,[1,2] the recognition of some autoinflammatory PSD with low incidence in general population is particularly challenging at a clinical level.[3–6] First, the clinical picture may show equivocal features and/or overlapping between different PSD; second, clinical manifestations are altered by local/systemic treatments masking the pathognomonic clues; third, the clinical history may be

not helpful. Moreover, although pustules represent the unifying clinical feature of these disorders, they may not always be the predominant finding, or they can be absent or not fully developed if the lesion is biopsied too early/too late.[7] Finally, there is a variety of PSD that share a high degree of clinical-morphological similarity but have rather different aetiology, either viral, bacterial, fungal, drug-induced or autoinflammatory, thus requiring timely and divergent therapeutic protocols.[3–7] To date, only the histopathologic examination enable clinicians to confirm the diagnostic suspect in front of a given PSD. Thus, having the possibility to use an *in vivo* non-invasive method able to simulate virtual histology would be very helpful in reducing the diagnostic time for laboratory.

The line-field confocal optical coherence tomography (LC-OCT) is a recently developed imaging technique able to perform a non-invasive, *in vivo*, examination of the epidermis and upper dermis, reaching very high image resolution and virtual histology.[8–19] The device is based on a supercontinuum laser, that, briefly, combines the technological advances of reflectance confocal microscopy (RCM) and optical coherence tomography (OCT) in terms of cellular and spatial resolution and vertical/horizontal navigation. Our group has successfully used LC-OCT to investigate the morphology of epidermis and adnexal structures in both healthy skin,[8] skin cancers and their simulators,[9–11] vesicobullous[12] and inflammatory conditions,[13] rare epidermal diseases[14–17] and uncommon paediatric conditions.[18,19] The accuracy of RCM in characterizing pustular rashes was previously demonstrated by Debarbieux *et al.*,[7] while standard OCT was employed to characterize *Malassezia* folliculitis pustules,[20] and dermoscopy was employed to imagine acute severe erythemato-pustular rashes.[21]

In this preliminary descriptive study, we aimed to investigate, for the first time, the potentialities and usefulness of the LC-OCT device in the non-invasive differential diagnosis of a series of PSD of the adult having different aetiologies, body location, microscopic features and incidence rates.

Materials and methods

Study population

Patients with suspected PSD were hospitalized between January 2018 and September 2021 in the inpatient Dermatology Departments of Siena University Hospital (Italy) or Saint-Etienne University Hospital (France). Inclusion criteria for the study were: definite diagnosis based on histopathological examination with/without direct immunofluorescence and presence of good quality LC-OCT images/videos/3D reconstruction. This study was realized in accordance with the Declaration of Helsinki; ethics committee approval was waived because the study affected neither routine diagnostic nor therapeutic management; all data were de-identified before use.

LC-OCT image acquisition protocol

The CE-marked *DeepLive* device (DAMAE Medical®, Paris, France) was used by two investigators expert in LC-OCT (LT, JLP). A drop of paraffin oil was applied to the tip of the hand-held probe before application to the skin, as previously described.[12] In *frame acquisition mode*, the device can obtain *in vivo and real time* images with 1.2-µm axial resolution/500-µm penetration depth/1.2-mm lateral field, in two modalities: in 2D mode, it acquires both vertically oriented and horizontally oriented images (10 frames/s); in 3D mode, it acquires a stack of horizontal images from the skin surface with steps of 1 µm. Using the *video mode*, the device can acquire up to 26 frames/s (basic mode), 16 frames/s (high-definition mode) or 8 frames/s (ultrahigh-definition mode). For each patient, sequential multiple LC-OCT examination including 2D, 3D and video was performed at presentation time over 3–5 recently appeared lesions at 3 body sites (i.e. centre of the lesion, lesion margin, perilesional skin – i.e. 1.5 cm from the pustule). For comparison, corresponding contralateral healthy sites were also imagined with 2D mode. A 6-mm self-adhesive paper reinforcement ring was used to ensure the correct position of the probe before imaging.[7–9] Each examination was performed by applying minimal to no pressure on the skin in order to ensure a correct visualization of the stratum corneum.[12]

Dermoscopic image acquisition protocol

When using the *in vivo* mode, the LC-OCT is able to simultaneously image the examined area with the integrated polarized dermoscopy 15× lens. The dermoscopic examination field correspond to a circular surface of 2.5 mm diameter at a 5-µm resolution; the red line inside corresponds to the vertical plane examination field of the LC-OCT laser, of 1.2 mm width. (Figs. 1–6).

Laboratory analyses

After LC-OCT examination, biopsy specimens for histopathologic analysis were performed with 4–6 mm punch biopsy at lesional margin. For each case, histopathologic slides were collected after pathology laboratory assessments and photographed (CM, LT, FF) by means of an optical microscope connected to a *AxioCam Zeiss* camera. According to clinical suspect, perilesional biopsy for DIF assay was required: the test was carried out and image acquired as previously described.[12]

LC-OCT images: Postprocessing and reading study

Postprocessing on LC-OCT images was performed for selected cases using software elaboration (*MinIP, 3DSlicer, version 4.10.2*) to realize a 'virtual biopsy', that is a 3D rectangular reconstruction of the skin (1.2 × 0.5 × 0.5 mm; Fig. 7e); the software elaboration also allows to virtually navigating inside the rectangle following the 3 axes, to measure stain- specific cells/structures. A selection of the best quality 2D images +3D

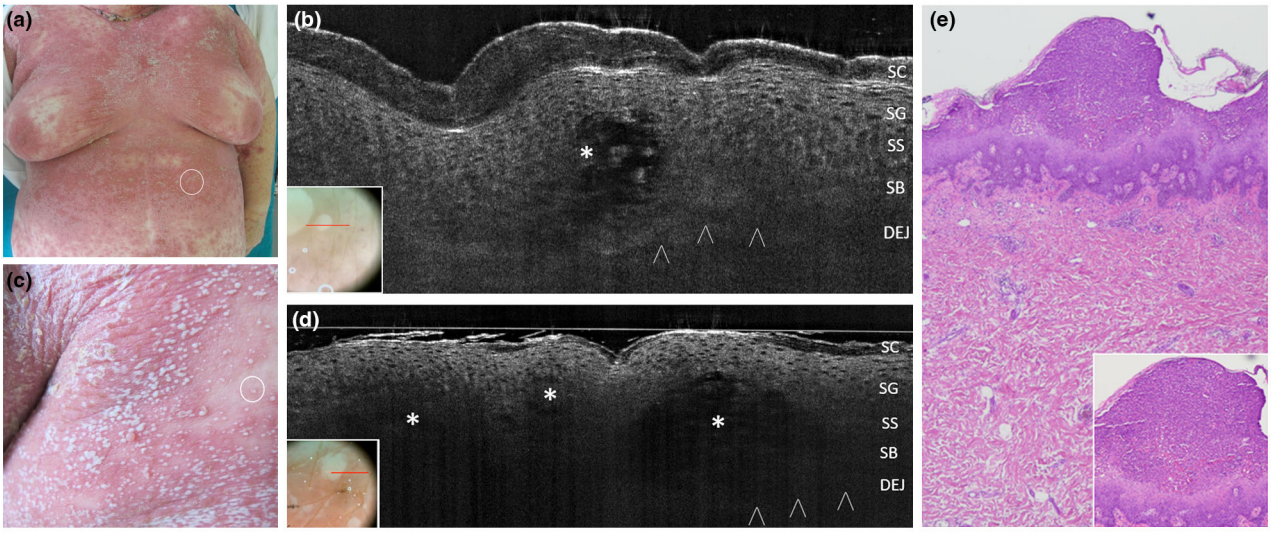

Figure 1 Acute Generalized Exanthematous Pustulosis from clarithromycin in a 65-year-old woman: clinical appearance at presentation time, with a 24-h pustular rash involving the whole trunk and proximal extremities (a,d). *In vivo* 2D LC-OCT of a tiny pustule of the abdomen (a, white circle) revealed an intraepidermal hypo-reflective area with ill-defined borders (asterisk) with floating large cells corresponding to neutrophils (b). Examination of multiple confluent on the upper back (c, white circle) revealed adjacent hypo-reflective areas with ill-defined borders (d, asterisks). Corresponding histopathologic examination, haematoxylin-eosin, OM 40× (e) and 100× (e, box) showing a intraepidermal pustule with a mixed inflammatory infiltrate of neutrophils and eosinophils in the underlying dermis [SC, stratum corneum; SG, stratum granulosum; SS, stratum spinosum; DEJ, dermal-epidermal junction; PD, papillary dermis; arrowheads: DEJ profile. The red line inside polarized dermoscopy 15× (c/d, box) corresponds to the LC-OCT vertical frame].

reconstructions was performed by 3 investigators (EC, LT, JLP). A total of 20 selected lesional LC-OCT images (15 LC-OCT 2D images and 5 3D LC-OCT images) associated with the corresponding dermoscopic images for each case was submitted to 4 investigators from the study group for blinded reading (MS, PR, EC, FF): they were asked to assess the presence/absence of pustular lesion inside a given frame, the depth of localization and the shape (uni/multilocular) of the pustule, the presence/absence of cell populations inside the pustule, the presence/absence of dilated vessels and inflammatory infiltrate in the papillary dermis. Any disagreement within the two investigator groups was solved by consensus among them (3 out of 4).

Results

Study population

The study included a total of 19 patients presenting with a several PSD with equivocal or overlapping clinical features characterized by different aetiology (drug-induced, inflammatory, autoinflammatory, viral), location (diffuse/multifocal/localized) and diverse incidence rates. They received 11 different histologic diagnosis of: Acute Generalized Exanthematous Pustulosis – AGEP (2); Generalized pustular psoriasis – GPP (2); Generalized pustular figurate erythema – GPFE (2); Subcorneal Pustular Dermatosis – SPD (1); Intraepidermal IgA pustulosis – IAD (2); Palmoplantar pustulosis – PPP (2), Palmoplantar pustular psoriasis – PPPP (2); Acrodermatitis continua of Hallopeau – ACH (1); herpetic whitlow – HW (2); vesico-pustular variant of Sweet syndrome – SSvp (1); vesico-pustular variant of Eosinophilic cellulitis – ECvp (2). Patients were 10 females and 9 males, aged between 35 and 79 years: on average, they were hospitalized after 1.1 months from the first skin manifestations onset. Pair comparison were set up as follows: AGEP vs. GPP vs. GPFE; SPD vs. IAD; PPP vs. HW; PPPP vs. ACH; SSvp vs. ECvp.

LC-OCT, dermoscopic and histologic findings

In Table 1 are reported and compared the peculiar characteristics of the pustules in the examined PSD, including: the distribution (body/hand, diffuse/localized/multifocal), the location (subcorneal/intraepidermal/junctional/subepidermal), the structure (unilocular /multilocular/coalescent), the morphology (shape/margin definition/content). The LC-OCT features and histologic findings are also reported. Each condition is then specifically discussed below, along with clinical history, dermoscopic features and differential diagnoses.

Acute generalized exanthematous pustulosis Patients with AGEP have a sudden onset of extensive skin rash rapidly covered with pustules with fever, raised inflammatory markers and peripheral leukocytosis (Table 1).[22,23] The main differentials are

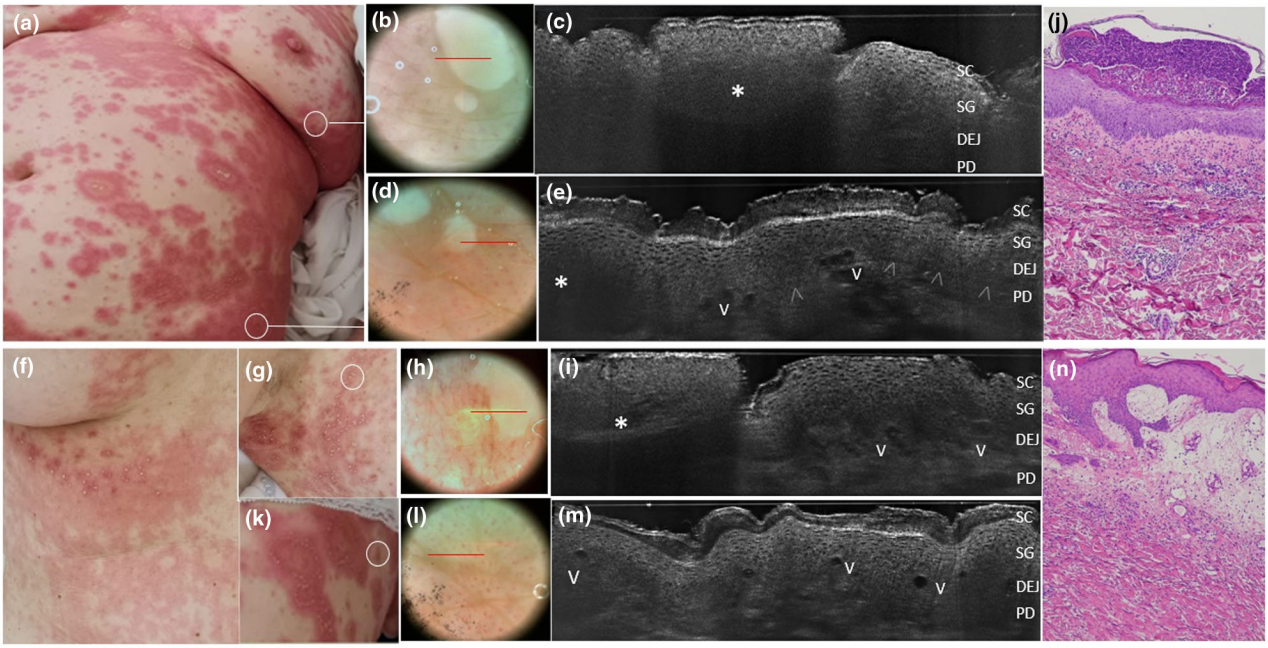

Figure 2 Generalized pustular figurate erythema in women aged 57 years (a-e) and 50 years (f-n) triggered by hydroxychloroquine. Clinical examination reveal annular to polycyclic erythematous-oedematous plaques distributed on the trunk, proximal extremities and flexural areas in both cases (a, f, g). Under *in vivo* 2D LC-OCT examination performed at lesional margins form both patients (c,i), pustules appeared as intraepidermal (c) or subcorneal (i) areas of roundish shape, well-defined borders and hyper-reflective homogenous content due to a dense neutrophils collection (asterisks) generating a posterior shadow. Dilated vessels are visible as black a-reflective areas (V) in perilesional skin (k) along with papillary dermal vessels and spongiosis (e, m). Matched histology showing a subcorneal pustule (l, haematoxylin-eosin, OM 40×) and a perilesional skin with edematous papillary dermis with ectatic vessels and inflammatory cells (n, haematoxylin-eosin, OM 100×). Papillary vessels correspond to the red dots seen in dermoscopy (e, m) [SC, stratum corneum; SG, stratum granulosum; DEJ, dermal-epidermal junction; PD, papillary dermis; V, capillary vessels; arrowheads: DEJ profile. The red line inside polarized dermoscopy images 15× (b/e/i/o, box) corresponds to the LC-OCT vertical frame].

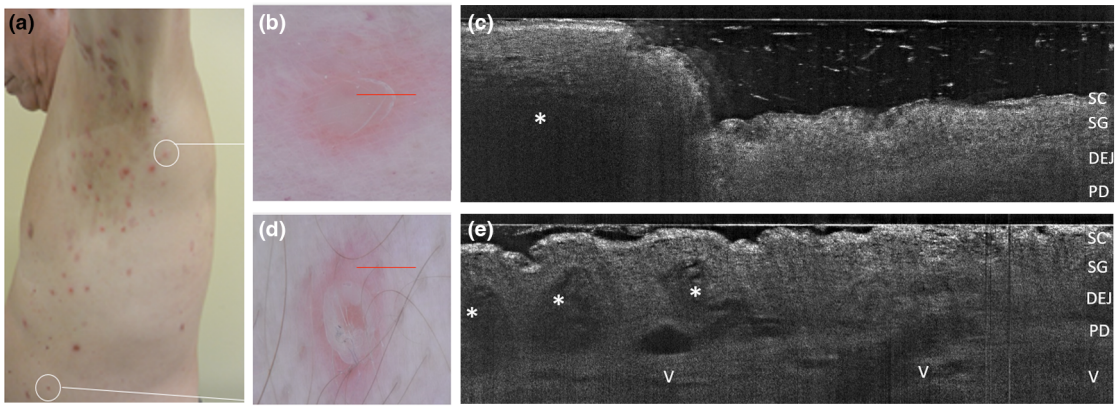

Figure 3 Subcorneal pustular dermatosis in a 63-year-old man (a). Combined dermoscopic (b,d) and LC-OCT (c,e) examinations of two recently developed lesions on the left axilla (b,c) and on the left side (d,e). *In vivo* 2D LC-OCT highlighted a large unilocular subcorneal pustule with well-defined borders (c, asterisk) and dense homogenously hyper-reflective content due to neutrophils accumulation and posterior shadow, as well as multilocular adjacent pustules in the upper epidermis (f, asterisks) with floating large cells corresponding to neutrophils. Vessels can be seen in the papillary dermis (f). [SC, stratum corneum; SG, stratum granulosum; DEJ, dermal-epidermal junction; PD, papillary dermis; V, capillary vessels. The red line inside polarized dermoscopy 15× (b, d) corresponds to the LC-OCT vertical frame].

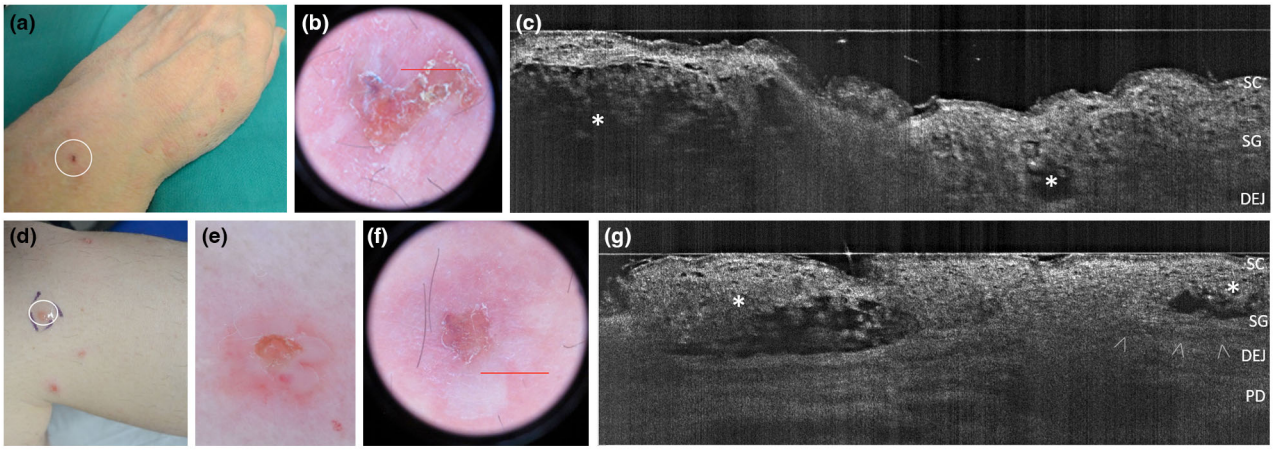

Figure 4 Clinical, dermoscopic and LC-OCT appearance of Intraepidermal IgA pustulosis (IAD) lesions in two women, one aged 61 years with the *Subcorneal Pustular Dermatosis-like* variant (IAD-*SPD*) (a-c) and one aged 42 years with the *Intraepidermal neutrophilic IgA dermatosis-like* variant (IAD-*IEN*) (d-g). *In vivo* 2D LC-OCT reveals two upper-epidermal spongiotic-multilocular pustules with ill-defined borders (c, asterisks) in IAD-SPD, while intraepidermal unilocular pustules with well-defined borders (g, asterisks) in IAD-IEN variant. [SC, stratum corneum; SG, stratum granulosum; DEJ, dermal-epidermal junction; arrowheads: DEJ profile; PD, papillary dermis. The red line inside polarized dermoscopy 15× (b, f) corresponds to the LC-OCT vertical frame].

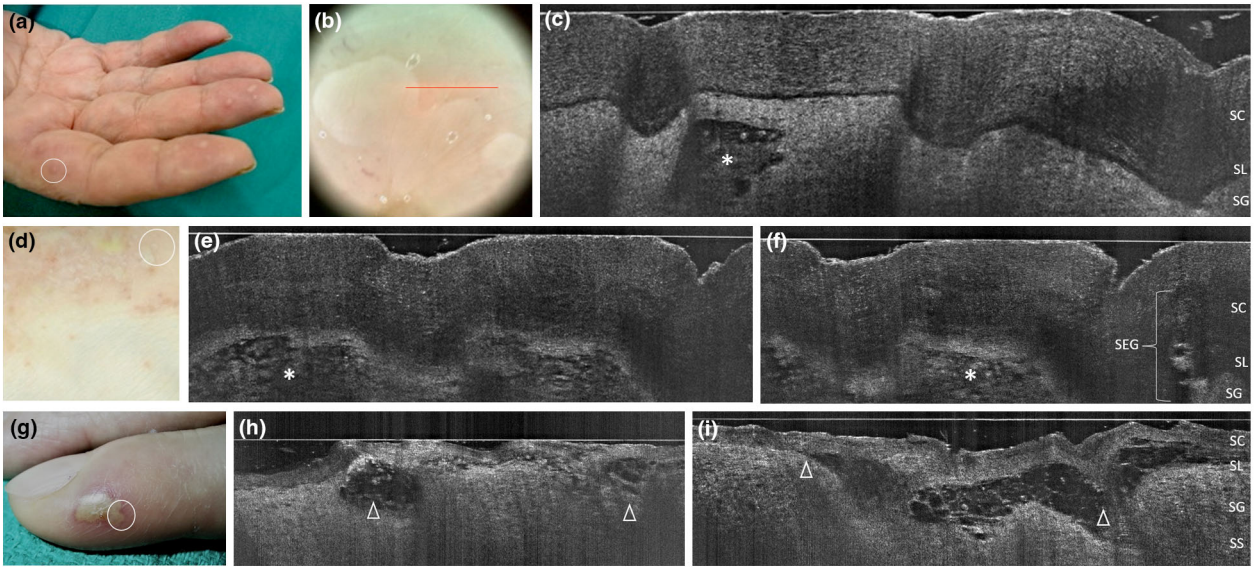

Figure 5 Palmoplantar pustulosis in two women aged 58 (a-c) and 39 years (d-f): clinical, dermoscopic and LC-OCT appearance of early developed lesions of the fingers; LC-OCT examination of a tiny recently developed pustule demonstrates an upper-epidermal area with well-defined borders and hyper-reflective roundish structures corresponding to neutrophils (c, asterisk), while examination of 7-days pustules of the plantar surface demonstrate multilocular spongiform hyporeflective areas with less-defined borders, filled with neutrophils (e, i, asterisks) and preserved SEG. Comparison with an herpetic whitlow case of a 45-year-old female (g-i): multilobated vesico-pustules are subcorneal, with cleavage level at SL (h,i, triangles), borders are ill-defined, and the content is not homogenous (hyper-reflective ridge made of branches of intercellular material, floating little roundish structures corresponding to necrotic keratinocytes) as a result of viral cytopathic effect. [SC, stratum corneum; SL, stratum lucidum; SG, stratum granulosum; SEG, sweat eccrine gland. The red line inside polarized dermoscopy 15× (b) corresponds to the LC-OCT vertical frame].

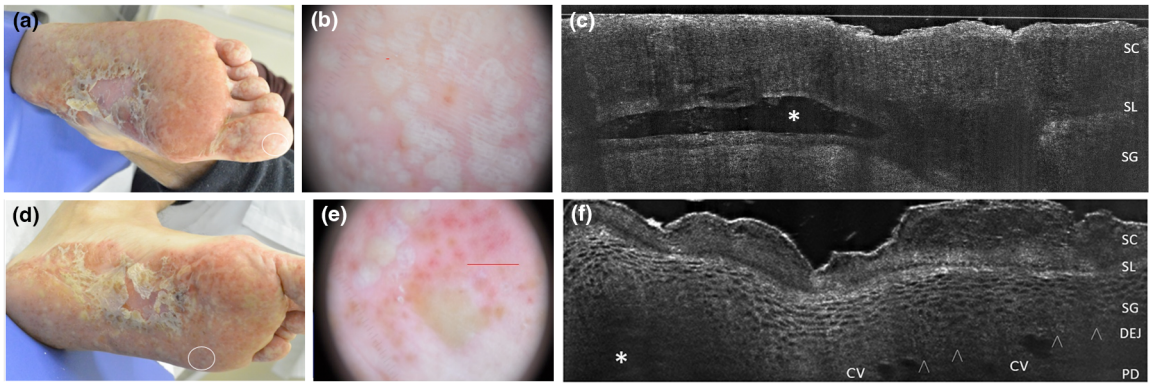

Figure 6 Palmoplantar pustular psoriasis of acute onset in a 38-year-old man. Clinical, dermoscopic and LC-OCT appearance of early developed lesions of finger toe (a), visible as white-yellowish roundish structure under dermoscopy (b) and as an upper-epidermal area with well-defined borders and hyper-reflective roundish structures corresponding to neutrophils in LC-OCT (c, asterisk). The LC-OCT examination carried out at plantar perilesional site (d, white circle) performed near a plantar pustule (f, asterisk) demonstrates the presence of well-defined large capillary loops in the papillary dermis (f), corresponding to the red clots (e) visible in the dermoscopic image [SC, stratum corneum; SL, stratum lucidum; SG, stratum granulosum; DEJ: dermo-epidermal junction; arrowheads: DEJ profile; CV: capillary vessels; harrowheads: dermo-epidermal junction. The red line inside polarized dermoscopy 159 (b) corresponds to the LC-OCT vertical frame].

GPP – which is sometimes associated with a positive history of psoriasis – and GPFE.[4,5,24] *In vivo* LC-OCT revealed uni or multilocular pustular lesions, either intraepidermal or subcorneal, as roundish/irregular in shape moderately hypo-reflective areas interrupting the epidermal structure, characterized by ill-defined margins. The content of pustules consisted of multiple floating moderately hyper-reflective roundish structures corresponding to inflammatory cells (Fig. 1): software segmentation and detailed analysis of selected frames revealed that irregular roundish elements showing different density signal between the centre – nucleus – and the periphery – cytoplasm – corresponded to neutrophils (~18–14 μm diameter), whereas round elements that are homogenously and moderately hyper-reflective corresponded to eosinophils (~10–14 μm diameter).[12] Dermoscopy did not reveal distinct vessels (as in GPFE) within the white-yellowish globules corresponding to pustules.[21]

Generalized pustular figurate erythema Recently described in response to hydroxychloroquine[25–27] GPFE is characterized by millimetric non-follicular subcorneal or intraepidermal pustules arising on the top of oedematous erythematous polycyclic to annular plaques (Table 1). In line with histologic findings from literature cases and from the two present cases, LC-OCT revealed dense subcorneal and intraepidermal unilocular neutrophilic pustules, edematous papillary dermis with multiple dilated capillary vessels, well visible as red dots under dermoscopy (Fig. 2).

Subcorneal pustular dermatosis Also known as Sneddon-Wilkinson disease, SPD typically involves the flexural areas with recurrent eruptions of tiny fragile pustules that coalesce rapidly to form annular, circinate or serpiginous patterns (Table 1).[28,29] The differential diagnosis is posed with IAD- SPD variant and Darier and Hailey–Hailey disease. *In vivo* 2D LC-OCT highlighted both unilocular subcorneal and multiple adjacent to coalescent upper-epidermal pustules, characterized by oval to round shape, well-defined borders, filled with neutrophils; moderately dilated capillary vessels are visible in the papillary dermis (Fig. 3).

Intraepidermal IgA pustulosis Recently included in the group of the neutrophilic dermatoses as IgA deposits in the upper epidermis are supposed to trigger an intense neutrophilic accumulation,[4,30,31] encompasses a spectrum of variants, the more common being the Subcorneal pustular dermatosis (SPD)-variant and the Intraepidermal neutrophilic dermatosis (IEN)-variant (Table 1). The IAD-SPD variant can affect flexural areas (dd with SPD) or the trunk/extremities where it assume an eczematiform appearance and circinate disposition. LC-OCT revealed multilocular subcorneal spongiotic pustules with ill-defined borders (Fig. 4a-c). The IAD-IEN variant typically shows sunflower-like lesions characterized by central crust surrounded by a ring millimetric fragile vesico-pustules (dd with dermatitis herpetiformis):[4,30,31] 2D LC-OCT revealed intraepidermal unilocular pustules with well-defined borders (Fig. 4d-g).

Palmoplantar pustulosis and herpetic whitlow PPP is characterized by white-yellowish pustules that rapidly appear on normal palmar/plantar skin, then turn yellow-brownish and coalesce within a background erythema, associated with itch/

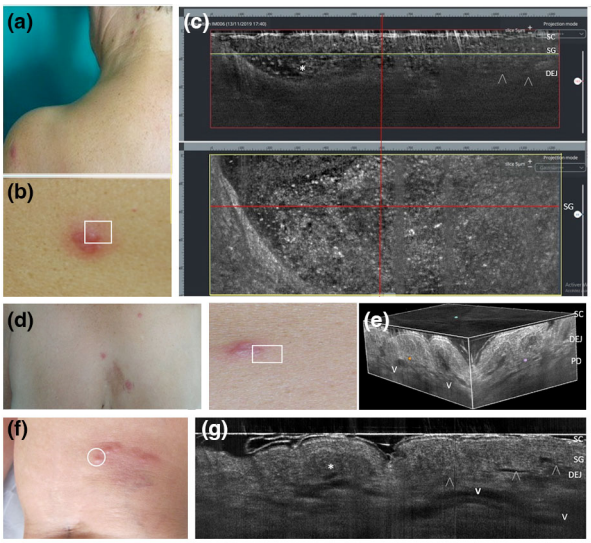

Figure 7 Sweet syndrome with vesicopustular appearance and multifocal lesion distribution in two women aged 62 (a–c) and 55 years (d–e). Combined vertical and horizontal LC-OCT frames (c) of a scapular lesion (b) revealed dense roundish a-reflective area with well-defined borders filled with multiple floating hyper-reflective roundish structures (c, asterisks), corresponding to neutrophilic collections in the epidermis and upper dermis (d); 3D LC-OCT of a chest lesion (d) showed the distribution of dilated vessels (e, V) and the presence of papillary oedema as hypo-reflective spaces in the dermis. Differential diagnosis with a case of eosinophilic cellulitis with papulo-pustular appearance in a 58-year-old woman (f), where LC-OCT shows an intraepidermal area with dense non-homogenous content in the epidermis/DEG (i, asterisk) corresponding to a non-homogeneous collection of eosinophils and neutrophils, overlying dilated tortuous vessels (g, V) in the whole dermis. [SC, stratum corneum; SL, stratum lucidum; SG, stratum granulosum; DEJ: dermo-epidermal junction; arrowheads: DEJ profile; V: vessels. The horizontal yellow line in the vertical LC-OCT frame (c, red box) indicate the depth level of the horizontal frame (c, yellow box) within the SG].

burning sensation (Table 1).[32–34] LC-OCT identified subcorneal/upper epidermal multilocular pustules surrounded by spongiform changes and unaltered sweat eccrine glands (Fig. 5a-f). The main clinical mimicker is PP (see below), herpetic whitlow and pityriasis rubra pilaris. LC-OCT examination of herpetic whitlow lesions revealed a subcorneal vesico-pustule with cleavage at stratum lucidum, showing the signs of viral cytopathic effect (i.e. multiple floating necrotic keratinocytes, hyper-reflective ridge made up by intercellular material branches (Fig. 5g-i). Another differential is pityriasis rubra pilaris, where however the papules are follicular, hyperkeratotic and evolve into pustules that extend to the dorsum of hands/feet.

Palmoplantar pustular psoriasis and Acrodermatitis continua of Hallopeau This localized chronic condition usually presents with eroded pustules/yellowish crusts within over an erythematous background with large scales.[2,3,33–35] *In vivo* 2D LC-OCT examination highlighted subcorneal confluent pustules with well-defined margin and floating neutrophils, cleavage at the stratum lucidum, as well as typical dilated capillary loops at perilesional site, corresponding to red clots under dermoscopy (Fig. 5) and pathognomonic in histologic section (Table 1).[2,3,33–35] Differentials include PPP, that however shows a less inflammatory background and is persistent (>3 months); GPP, which is indeed not limited to palmar and plantar surfaces but rapidly spreads all over the body surface and can either be a relapsing or persistent;[36] ACH at first stage or associated PPPP/ACH cases.[3] However, the ACH course reveals a more aggressive trend with progressive destruction of skin and nail of the involved phalanx.[2,3,15] Of converse, we previously reported that *in vivo* LC-OCT examination in ACH lesion of the fingers was able to detect irregular keratinocytes, altered dermoepidermal junction and tortuous dilated vessels, also visible in dermoscopy as a polymorphous pattern.[15]

Sweet syndrome and Eosinophilic cellulitis – vesicopustular variants This condition can manifest without fever and multifocal/localized pseudovesicular erythematous papulo-vesicles then evolves into pustules or plaques with dense dermal neutrophilic infiltrate (Table 1) suggesting an overlap between superficial and deep neutrophilic infiltration.[6,37–39] LC-OCT examination at lesional sites revealed dense homogenous neutrophilic collections with well-defined borders extending from the epidermis to the papillary dermis, dilated vessels and papillary oedema sings suggesting intense inflammation extending to nearly perilesional examination points (Fig. 7a-g). Clinically, a differential diagnosis with uncommon EC subtypes: however, subcorneal pustules are composed by either neutrophils and eosinophils, suggesting a primary eosinophilic response to an external antigen that triggers and amplifies a neutrophilic tissue response.[40,41] In this case, LC-OCT highlights a dense intraepidermal papule extending to the dermal–epidermal junction, with no clearly visible neutrophils, and overlying intensely dilated tortuous vessels in the whole dermis (Fig. 7h-i).

Discussion

This preliminary descriptive study was carried out to investigate, for the first time, the potentiality and usefulness of a new non-invasive imaging device in the differential diagnoses of PSD with similar clinical appearance. We compared together PSD forms with diffuse body distribution (e.g. AGEP vs. GPP vs. GPFE), forms with multifocal body distribution (e.g. IAD vs. SPD, or SS vs. EC), forms with localized hand and/or palmoplantar distribution (e.g. PPPP vs. ACH, PP vs. HW). By using *in vivo* 2D LC-OCT, we were able to visualize, *real time* and at bed-side, the location (subcorneal/intraepidermal/junctional/sub-epidermal), structure (uni/multilocular/coalescent), morphology (shape,

Table 1 Clinical and microscopic characteristics of a series of pustular skin disorders and their clinical mimickers

Condition	Pustule distribution	LC-OCT features of pustules			Histologic features
		Composition	Location, structure	Morphology	
AGEP	Body, diffuse	Eosinophils (+++), neutrophils (+)	Subcorneal (+)/ intraepidermal (+); multilocular (++)/confluent (+)	Irregular shape, ill-defined border, moderately hyper-reflective not homogenous content	Focal dyskeratosis, possible necrotic keratinocytes, focal spongiosis, mixed interstitial and mid-dermal infiltrates, papillary dermis oedema, fibrinoid deposition
GPP	Body, diffuse	Neutrophils (+++), lymphocytes (+)	Subcorneal (++), unilocular (+)	Roundish shape; well-defined borders, homogenous content	Acanthosis, suprapapillary thinning, dilated vessels in papillary dermis, mixed lymphoistiocytic dermal infiltrates + spare neutrophils
GPFE	Body, diffuse	Neutrophils (+++), eosinophils (+)	Intraepidermal (++)/subcorneal (+); multilocular (++)/ unilocular (+)	Roundish shape, well-defined borders, highly hyper-reflective homogenous content	Mild focal acantholysis, exocytosis, spongiosis, papillary dermis oedema, perivascular lymphocytic infiltrate (neutrophils, eosinophils, mast cells)
SPD	Body, multifocal	Neutrophils (+++), eosinophils (0/+)	Subcorneal (++)/upper-epidermal (+); unilocular (++)/confluent	Roundish shape, well-defined borders, hyper-reflective homogenous or not content	Normal epidermis (or rare focal acantholysis), moderate periadnexal mixed lymphoistiocytic superficial dermis infiltrates subcorneal neutrophils
IAD *SPD-like*	Body, multifocal	Neutrophils (+++)	Sub-corneal; multilocular	Irregular shape; ill-defined border; not homogenous content	Mild or no acanthosis, central crusting, surrounding flaccid vesicles/pustules, cell surface iga deposits in the upper epidermis
IAD *IEN-like*	Body, multifocal	Neutrophils (+++)	Intraepidermal unilocular (+)	Roundish shape; well-defined borders, not homogenous content	Central crusts and peripheral ring of tiny vesico-pustules, cell surface iga deposits in the epidermis
PPP	Palms and/or soles, localized	Neutrophils (+++), lymphocytes (+)	Intraepidermal (++)/subcorneal (+); multilocular (+)	Irregular/roundish shape; well-defined borders, not homogenous content	Surrounding spongiform changes; Preserved spiral shape of the eccrine gland ducts
PPPP	Palms and/or soles, localized	Neutrophils (+++), lymphocytes (+)	Sub-corneal (++); unilocular (+), confluent (++)	Roundish shape; well-defined borders, homogenous content	Perifollicular hyperkeratosis, acanthosis, parakeratosis, suprapapillary thinning, dilated vessels in papillary dermis, mixed lymphoistiocytic dermal infiltrates, altered spiral shape of eccrine ducts
SS	Body, diffuse	Neutrophils (+++)	Intraepidermal (+)/ junctional (+)//subepidermal (++)	Irregular shape; well-defined borders, homogenous content	Epidermal spongiosis, dense neutrophilic infiltrate in the dermis extending to the epidermis, possible papillary oedema
EC	Body, localized	Eosinophils (++), neutrophils (+)	Intraepidermal/ junctional	Irregular shaped papule, ill-defined borders, non-homogenous content	Papillary dermal oedema, mixed eosinophilic-neutrophilic infiltrate in the upper-mid, no signs of vasculitis

Table 1 *Continued*

Condition	Pustule distribution	LC-OCT features of pustules			Histologic features
		Composition	Location, structure	Morphology	
ACH	Hand/palms, localized	Neutrophils (+++)	Subcorneal, unilocular (+), confluent (+++)	Irregular shape; ill-defined borders, non-homogenous content	Adjacent spongiform pustules of Kogoj or aggregates of leukocytes, altered dermal-epidermal junction and keratinocytes, tortuous dilated vessels in the papillary dermis
HW	Hand, palms localized	Necrotic keratinocytes (+++), intercellular material (++), neutrophil (+)	Subcorneal, multilobated (+), confluent	Roundish shape; well-defined borders, non-homogenous content	Cytoplasmatic/nuclear inclusions, acantholysis, intraepidermal blister/vacuolation in the cytoplasm along basal keratinocytes, inflammatory infiltrate is mixed, predominantly lymphocytes and neutrophils with scattered eosinophils

ACH, Acrodermatitis continua of Hallopeau; AGEP, Acute Generalized Exanthematous Pustulosis; ECvp, Eosinophilic cellulitis vesico-pustular variant; GPFE, Generalized pustular figurate erythema; GPP, Generalized pustular psoriasis; HW, Herpetic whitlow; IAD, Intraepidermal IgA pustulosis, variants: SPD-like; IEN-like, intraepidermal neutrophilic IgA dermatosis; PPP, Palmoplantar pustulosis; PPPP, Palmoplantar pustular psoriasis; SPD, Subcorneal Pustular Dermatosis; SSvp, Sweet syndrome -vesico-pustular variant.

margin definition) and content of pustular lesions in each one of the examined patients by applying the probe over a selected lesion or in perilesional sites. (Table 1, Figs. 1–6) Concerning pustules' location, some PSD forms appeared mainly subcorneal (SPD, ACH), upper-epidermal (GPFE, IAD-SPD, PPPP, GPP), intraepidermal (AGEP, GPFE, IAD-IEN, PPP, HW), junctional/subepidermal (EC) or subepidermal/papillary dermis (SS).[1–7] Considering the pustules' composition, the majority of cases had a prevalent neutrophilic component[2–6] while some conditions exhibit a relevant and/or pathognomonic eosinophilic component (AGEP, GPFE, EC).[22–27,40,41] Moreover, it was possible to detect clinically invisible changes in perilesional or distant skin, such as vascular alterations, dense inflammatory infiltrate or initial intraepidermal pustule formation.

The examination was generally rapid, taking 1 s for single frameshot, approximately 15 s for a vertical scan (i.e. automatic acquisition of stacks) and generally less than 5 min for a combined lesion examination, if the probe is correctly positioned on the lesional margin or another examination site. Of note, if the probe was maintained stable during image acquisition, no further imaging postprocessing was necessary. Another advantage is the possibility to acquire video and 3D stack even in anatomically difficult areas such as the skin folds – axillae, groin, interdigital areas – or areas whit soft and thick underlying subcutaneous tissues (e.g. abdomen, scrotum, dorsum in obese person). thanks to the small tip of the probe (1.5 cm) and to the automatic focus of the device that adapt the laser signal according to the density of the examined surfaces .

Comparison with dermoscopic pictures associated to each LC-OCT frame was also carried out: the integrated 15x polarized dermoscopic lens demonstrated to visualize correctly the pustular structure, the dilated vessels in papillary dermis, the presence of large hyperkeratosis alteration and of background erythema. In particular, having a clear correspondence between the red line of the dermoscopic window and the LC-OCT frame enable us to easily navigate within these millimetric lesions without losing the right orientation. The correlation among structures' morphology and level visualized in LC-OCT frames and in associated dermoscopic frames was judged as excellent by expert consensus (Figs. 1–6).

The combined evaluation of the LC-OCT findings and the corresponding histologic pictures was performed by experts and an adequate correlation level was assessed. Analysing the 3D combination of multiple horizontal and vertical frames of a given lesional area allowed us to see a sort of 'virtual biopsy' of the respecting the real morphology of the skin layers, cellular components, adnexal, dermal and vascular structures. Indeed, there is a consensus that *in vivo* LC-OCT examination gives back an 'original view' of a selected skin area, not affected by stretching pressures or artefacts that are impossible to avoid during histologic slide preparation.

This study structure has some limitations. The main current limitation of the DeepLive® device is the impossibility to mark a specific cell population in an *ex-vivo* manner being not equipped to realize a specific marking with fluorescent autoantibodies. At present, the device/software equipment allows to realize the 'segmentation' (i.e. measurement detection and virtual

stain) of a specific cell population (e.g. erythrocytes, neutrophils) or a specific structure (e.g. sweat eccrine glands, glomerular papillary vessels) based on the postprocessing elaboration of elements exhibiting the same refractory density (i.e. grey level), shape, morphology and location.[16] Hence (second point), an adequate preparation on LC-OCT image interpretation and correlation with dermoscopic and histologic findings is necessary. Third, the use of the device *in vivo* requires a certain degree of experience and dexterity: the training time depends on the operator previous experience with non-invasive imaging devices, but is shorter than that needed for RCM, being closer to high-resolution skin ultrasound and high-resolution videodermoscopy. Fourth, the sample size was too small to derive statistical analysis besides descriptive statistics; however, the collected case series is quite representative of PSD with difference incidence rates, which can be encountered in clinical practice and/or require hosptalization in dermatology inpatient departments.[1–6]

In conclusion, this new non-invasive, painless and rapid examination technique able to reach cell resolution, paired with dermoscopic indicator,[7,21] can be of help in visualizing the pustule morphology and/or alterations in the adnexa structure and/or changes in the upper/mid dermis, and orienting the diagnostic suspect in front of PSD with equivocal clinical appearance. Although further studies are necessary in the next future, this technology could also possibly used to monitoring the response to treatment by detection of microscopic changes in apparently healthy skin areas.

Aknowledgement

Maxime Cazalas, Damae Medical, Paris (France) for LC-OCT imaging editing. Open Access Funding provided by Universita degli Studi di Siena within the CRUI-CARE Agreement.

Consent

The patients in this manuscript have given written informed consent to the publication of their case details.

Data availability statement

The data that support the findings of this study are available from the corresponding author upon reasonable request.

References

1 James G, Miller MJJ. Pustules. In Marks JG, Miller JJ, eds. Lookingbill and Marks' Principles of Dermatology (Sixth Edition). Elsevier, Philadelphia, 2019: 166–183. ISBN: 9780323430401.
2 Mengesha YM, Bennett ML. Pustular skin disorders: diagnosis and treatment. *Am J Clin Dermatol* 2002; **3**: 389–400.
3 Bachelez H. Pustular psoriasis and related pustular skin diseases. *Br J Dermatol* 2018; **178**: 614–618.
4 Feldmeyer L, Hashimoto T, Borradori L. Superficial neutrophilic dermatoses: from subcorneal pustular dermatosis (Sneddon-Wilkinson disease) to intercellular IgA dermatoses. Neutrophilic Dermatoses 2018. Springer, Cham, 2018: 101–117.
5 Naik HB, Cowen EW. Autoinflammatory pustular neutrophilic diseases. *Dermatol Clin* 2013; **31**: 405–425.
6 Filosa A, Filosa G. Neutrophilic dermatoses: a broad spectrum of disease. *G Ital Dermatol Venereol* 2018; **153**: 265–272.
7 Debarbieux S, Depaepe L, Poulalhon N, Dalle S, Balme B, Thomas L. Reflectance confocal microscopy characteristics of eight cases of pustular eruptions and histopathological correlations. *Skin Res Technol* 2013; **19**: e444–e452.
8 Monnier J, Tognetti L, Miyamoto M *et al.* In vivo characterization of healthy human skin with a novel, non-invasive imaging technique: line-field confocal optical coherence tomography. *J Eur Acad Dermatol Venereol* 2020; **34**: 2914–2921.
9 Cinotti E, Tognetti L, Cartocci A *et al.* Line-field confocal optical coherence tomography for actinic keratosis and squamous cell carcinoma: a descriptive study. *Clin Exp Dermatol* 2021; **46**: 1530–1541.
10 Suppa M, Fontaine M, Dejonckheere G *et al.* Line-field confocal optical coherence tomography of basal cell carcinoma: a descriptive study. *J Eur Acad Dermatol Venereol* 2021; **35**: 1099–1110.
11 Lenoir C, Diet G, Cinotti E *et al.* Line-field confocal optical coherence tomography of sebaceous hyperplasia: a case series. *J Eur Acad Dermatol Venereol* 2021; **35**: e509–e511.
12 Tognetti L, Cinotti E, Suppa M *et al.* Line field confocal optical coherence tomography: an adjunctive tool in the diagnosis of autoimmune bullous diseases. *J Biophotonics* 2021; **14**: e202000449.
13 Tognetti L, Ekinde S, Habougit C *et al.* Delayed tattoo reaction from red dye with overlapping clinicopathological features: examination with high-frequency ultrasound and line-field optical coherence tomography. *Dermatol Pract Concept* 2020; **10**: e2020053.
14 Cinotti E, Santi F, Perrot JL, Habougit C, Tognetti L, Rubegni P. Squamous cell carcinoma arising on acrodermatitis continua of Hallopeau: clinical and noninvasive skin imaging features. *Int J Dermatol* 2021; **60**: 763–765.
15 Tognetti L, Fiorani D, Suppa M *et al.* Examination of circumscribed palmar hypokeratosis with line-field confocal optical coherence tomography: dermoscopic, ultrasonographic and histopathologic correlates. *Indian J Dermatol Venereol Leprol* 2020; **86**: 206–208.
16 Tognetti L, Rizzo A, Fiorani D *et al.* New findings in non-invasive imaging of aquagenic cheratoderma: line-field optical coherence tomography, dermoscopy and reflectance confocal microscopy. *Skin Res Tech* 2020; **26**: 956–959.
17 Tognetti L, Carraro A, Lamberti A *et al.* Kaposi sarcoma of the glans: new findings by line field confocal optical coherence tomography examination. *Skin Res Tech* 2020; **27**: 285–287.
18 Tognetti L, Carraro A, Cinotti E *et al.* Line-field confocal optical coherence tomography for non-invasive diagnosis of lichenoid dermatoses of the childhood: a case series. *Skin Res Technol* 2021; **27**: 1178–1181.
19 Tognetti L, Bertello M, Cinotti E, Rubegni P. Acquired digital fibrokeratoma: first observation by high-resolution skin ultrasound and line-field confocal optical coherence tomography. *Indian J Dermatol Venereol Leprol* 2022; **88**: 275.
20 Andersen AJ, Fuchs C, Ardigo M *et al.* In vivo characterization of pustules in Malassezia folliculitis by reflectance confocal microscopy and optical coherence tomography. A case series study. *Skin Res Technol* 2018; **24**: 535–541.
21 Errichetti E, Stinco G. Dermatoscopy in life-threatening and severe acute rashes. *Clin Dermatol* 2020; **38**: 113–121.
22 Szatkowski J, Schwartz RA. Acute generalized Exanthematous pustulosis (AGEP): a review and update. *JAAD* 2015; **73**: 843–848.
23 Feldmeyer L, Heidemeyer K, Yawalkar N. Acute generalized Exanthematous pustulosis: pathogenesis, genetic background, clinical variants and therapy. *IJMS* 2016; **17**: 1214.
24 Hoegler KM, John AM, Handler MZ, Schwartz RA. Generalized pustular psoriasis: a review and update on treatment. *J Eur Acad Dermatol Venereol* 2018; **32**: 1645–1651.

25 Schwartz RA, Janniger CK. Generalized pustular figurate erythema: a newly delineated severe cutaneous drug reaction linked with hydroxychloroquine. *Dermatol Ther* 2020; **33**: e13380.
26 Suarez-Valle A, Fernandez-Nieto D, Melian-Olivera A *et al*. Comment on "generalized pustular figurate erythema: a newly delineated severe cutaneous drug reaction linked with hydroxychloroquine": report of a COVID-19 patient with particular findings. *Dermatol Ther* 2020; **33**: e13852.
27 Abadías-Granado I, Palma-Ruiz AM, Cerro PA *et al*. Generalized pustular figurate erythema first report in two COVID-19 patients on hydroxychloroquine. *J Eur Acad Dermatol Venereol* 2021; **35**: e5–e7.
28 Cheng S, Edmonds E, Ben-Gashir M, Yu RC. Subcorneal pustular dermatosis: 50 years on. *Clin Exp Dermatol* 2008; **33**: 229–233.
29 Watts PJ, Khachemoune A. Subcorneal pustular dermatosis: a review of 30 years of Progress. *Am J Clin Dermatol* 2016; **17**: 653–671.
30 Tsuruta D. Intercellular IgA dermatosis. *Br J Dermatol* 2017; **176**: 13–14.
31 Hashimoto T, Teye K, Ishii N. Clinical and immunological studies of 49 cases of various types of intercellular IgA dermatosis and 13 cases of classical subcorneal pustular dermatosis examined at Kurume University. *Br J Dermatol* 2017; **176**: 168–175.
32 Misiak-Galazka M, Zozula J, Rudnicka L. Palmoplantar pustulosis: recent advances in etiopathogenesis and emerging treatments. *Am J Clin Dermatol* 2020; **21**: 355–370.
33 Freitas E, Rodrigues MA, Torres T. Diagnosis, screening and treatment of patients with palmoplantar pustulosis (PPP): a review of current practices and recommendations. *CCID* 2020; **13**: 561–578.
34 Yamamoto T. Similarity and difference between palmoplantar pustulosis and pustular psoriasis. *J Dermatol* 2021; **48**: 750–760.
35 Raposo I, Torres T. Palmoplantar psoriasis and palmoplantar pustulosis: current treatment and future prospects. *Am J Clin Dermatol* 2016; **17**: 349–358.
36 Navarini AA, Burden AD, Capon F *et al*. European consensus statement on phenotypes of pustular psoriasis. *J Eur Acad Dermatol Venereol* 2017; **31**: 1792–1799.
37 Villarreal-Villarreal CD, Ocampo-Candiani J, Villarreal-Martínez A. Sweet syndrome: a review and update. *Actas Dermosifiliogr* 2016; **107**: 369–378.
38 Feldmeyer L, Ribero S, Gloor AD, Borradori L. Neutrophilic dermatoses with unusual and atypical presentations. *Clin Dermatol* 2021; **39**: 261–270.
39 Sommer S, Wilkinson SM, Merchant WJ, Goulden V. Sweet's syndrome presenting as palmoplantar pustulosis. *JAAD* 2000; **42**(2 Pt 2): 332–334.
40 Kamiyama T, Watanabe H, Sueki H. Bullous eosinophilic cellulitis with subcorneal pustules. *Indian J Dermatol Venereol Leprol* 2015;**81**: 301–3.
41 Iinuma S, Takahashi C, Ishida-Yamamoto A. Eosinophilic cellulitis with pustular lesions. *Int J Dermatol* 2022; **61**: e227–e228.